Numerical exploration of L-functions: Dirichlet (abelian) and modular (GL(2))

Critical zeros, completed function, and coherence/confinement criteria

Adil HAJADI

September 10, 2025

Abstract

We present a numerical exploration of abelian L-functions (quadratic Dirichlet characters) and non-abelian ones (holomorphic weight-2 modular forms, $GL(2)$), with two goals: (i) to verify the alignment of zeros on the critical line $\Re(s) = \frac{1}{2}$ (*zeta-confinement*); and (ii) to analyze the phase/amplitude regularity of the completed function $\Lambda(s)$ (*zeta-coherence*). We describe the completion (conductor, gamma factors), the use of an approximate functional equation (AFE), the detection of zeros via a Hardy-type reading (for example $\operatorname{Im}\Lambda(1/2 + it)$ when the functional sign is -1), as well as numerical stability (truncation, precision, adaptive grid). In the end we compare these classical readings with internal model objects ($\mathscr{Z}_{\mathrm{coh}}()$, $\mathscr{Z}_{\mathrm{conf}}()$) only as qualitative controls, in order to keep the main anchoring in `math.NT`. *Plan*: context and aims; recalls on L-functions and completion; tested families (Dirichlet, GL(2)); methodology; numerical results and interpretation.

Contents

1 Context and aims

The aim is twofold: on the one hand to **verify numerically**, on prescribed height windows t, the alignment of zeros on the critical line $\Re(s) = \frac{1}{2}$ (GRH spirit), which we call *zeta-confinement*; on the other hand to **observe the regularity** of the oscillations of the completed function $\Lambda(s)$, interpreted as *zeta-coherence* (clean zeros, clear sign alternation, oscillations without unexpected singularities). These two criteria structure the experimental protocol and the visualizations (profiles $|L(1/2 + it)|$, Hardy-type reading, cumulative counting $N(T)$, local maps).

[11pt,a4paper]article

[utf8]inputenc [T1]fontenc [english]babel

amsmath,amssymb,amsthm,mathtools mathrsfs geometry microtype graphicx xcolor booktabs enumitem hyperref margin=2.7cm

Theorem [theorem]Proposition [theorem]Lemma [theorem]Definition [theorem]Remark [theorem]Example

Towards a Coherence Zeta

From Decimal Recurrences to Analytic Structures Adil HAJADI September 10, 2025

Abstract

We introduce and study a weighted variant of the classical Euler product, the *Coherence Zeta*, where each prime p is assigned an arithmetic weight derived from the period of the expansion of $1/p$ in base b. Writing $\mathrm{ord}_p(b)$ for the multiplicative order of b modulo p, we consider

$$\mathscr{Z}_{\mathrm{coh}}(s) \;=\; \sum_p \frac{1}{\mathrm{ord}_p(b)}\, p^{-s},$$

and discuss its links with Dirichlet series, the "wave" reading via $\sum_p \cos(t \log p)/\sqrt{p}$, as well as completions Ξ_{coh} satisfying a conjectural symmetry $s \leftrightarrow 1 - s$. We present the arithmetic framework (decimal periods $\leftrightarrow$ multiplicative orders), set the definitions and goals, and sketch numerical tests together with comparisons to ζ and classical L-functions.

Contents

2 Background: L-functions and completion

2.1 Dirichlet case (degree 1)

Let $\chi \pmod{q}$ be a primitive Dirichlet character. Define

$$L(s, \chi) \;=\; \sum_{n \geq 1} \frac{\chi(n)}{n^s}, \qquad \Re s > 1.$$

Let $a \in \{0,1\}$ be the parity determined by $\chi(-1) = (-1)^a$. The *completed* function is

$$\Lambda(s,\chi) \;=\; \Big(\frac{q}{\pi}\Big)^{\frac{s+a}{2}}\,\Gamma\Big(\frac{s+a}{2}\Big)\,L(s,\chi),$$

and it satisfies the functional equation

$$\Lambda(s,\chi) \;=\; \varepsilon_\chi\,\Lambda(1-s,\overline{\chi}), \qquad \varepsilon_\chi \;=\; \frac{\tau(\chi)}{i^{\,a}\sqrt{q}} \;=\; e^{i\phi_\chi}, \quad |\varepsilon_\chi| = 1,$$

where $\tau(\chi)$ is the Gauss sum and $\phi_\chi = \arg \varepsilon_\chi$. A Hardy-type real reading on the critical line uses

$$\theta_\chi(t) \;=\; \tfrac{1}{2}\arg\Gamma\Big(\frac{\frac{1}{2}+it+a}{2}\Big) \;-\; \frac{t}{2}\log\Big(\frac{\pi}{q}\Big) \;+\; \tfrac{1}{2}\,\phi_\chi, \qquad Z_\chi(t) \;:=\; e^{-i\theta_\chi(t)}\,\Lambda(\tfrac{1}{2}+it,\chi) \in \mathbb{R}.$$

Then the real zeros of $Z_\chi(t)$ coincide with the zeros of $L(s,\chi)$ on $\Re s = \frac{1}{2}$.

For computations we use a symmetric *approximate functional equation* (AFE):

$$L(s,\chi) \;=\; \sum_{n\le M} \frac{\chi(n)}{n^s} \;+\; X_\chi(s)\sum_{n\le M}\frac{\overline{\chi}(n)}{n^{\,1-s}} \;+\; \mathrm{Err}_\chi(s;M),$$

with

$$X_\chi(s) \;=\; \varepsilon_\chi\Big(\frac{q}{\pi}\Big)^{\frac{1}{2}-s}\,\frac{\Gamma\big(\frac{1-s+a}{2}\big)}{\Gamma\big(\frac{s+a}{2}\big)}, \qquad M \asymp C\sqrt{\frac{q(|t|+1)}{2\pi}},$$

and $s = \frac{1}{2}+it$; the constant $C > 0$ controls the truncation (chosen empirically for stability).

2.2 Holomorphic modular case (degree 2, $GL(2)$)

Let $f = \sum_{n\ge1} a_n\, n^{(k-1)/2} q^n$ be a holomorphic newform of weight $k = 2$, level N, trivial nebentypus (for simplicity). The normalized Dirichlet series is

$$L(s,f) \;=\; \sum_{n\ge1}\frac{a_n}{n^{\,s}}, \qquad \Re s > 1.$$

The completed function is

$$\Lambda(s,f) \;=\; N^{\,s/2}\,(2\pi)^{-s}\,\Gamma(s+\tfrac{k-1}{2})\,L(s,f) \;=\; N^{\,s/2}\,(2\pi)^{-s}\,\Gamma(s+\tfrac{1}{2})\,L(s,f),$$

and it satisfies

$$\Lambda(s,f) \;=\; \varepsilon_f\,\Lambda(1-s,f), \qquad \varepsilon_f \in \{\pm1\}.$$

On the critical line we read zeros via

$$\text{if } \varepsilon_f = -1: \quad \operatorname{Im}\Lambda(\tfrac{1}{2}+it,f) = 0, \qquad \text{if } \varepsilon_f = +1: \quad \operatorname{Re}\Lambda(\tfrac{1}{2}+it,f) = 0.$$

A symmetric AFE is used as in the Dirichlet case:

$$L(s,f) \;=\; \sum_{n\le M}\frac{a_n}{n^{\,s}} \;+\; X_f(s)\sum_{n\le M}\frac{a_n}{n^{\,1-s}} \;+\; \mathrm{Err}_f(s;M),$$

with

$$X_f(s) \;=\; \varepsilon_f\,N^{\,\frac{1}{2}-s}\,(2\pi)^{2s-2}\,\frac{\Gamma(2-s)}{\Gamma(s)}, \qquad M \asymp C\sqrt{N(|t|+1)}.$$

(Here we use the Hecke normalization so that $|a_p| \le 2$ for primes $p \nmid N$.)

2.3 Notes on numerical reading

Throughout, we:

- evaluate $|L(1/2+it)|$ on adaptive grids to reveal *deep minima*;
- detect zeros by sign changes of Hardy-type readings ($Z_\chi(t)$ or $\operatorname{Im}\Lambda$);
- control stability via $M = M(t)$, working precision, and comparison of forward/backward AFE sums.

Figures referenced later include: `dirichlet_profile_q7.png`, `arg_principle_q7.png`, and `gl2_profile_level11.png`.

3 Tested families and numerical protocol

3.1 Families under test

Dirichlet, quadratic mod 7. We take the primitive quadratic character χ mod 7 given by the Legendre symbol

$$\chi(n) = \left(\frac{n}{7}\right) = \begin{cases} 0, & 7 \mid n, \\ +1, & n \not\equiv 0 \bmod 7 \text{ and } n \text{ is a square mod } 7, \\ -1, & \text{otherwise.} \end{cases}$$

It has parity $a \in \{0,1\}$ with $\chi(-1) = (-1)^a$, Gauss sum $\tau(\chi)$ and functional sign $\varepsilon_\chi = \tau(\chi)/(i^a\sqrt{7})$. Zeros on $\Re s = \frac{1}{2}$ are read through a Hardy-type real quantity $Z_\chi(t) = e^{-i\theta_\chi(t)}\Lambda(\frac{1}{2}+it,\chi)$ (see Window 2).

Modular, holomorphic $GL(2)$ of level 11. We use the weight-2 newform of level $N = 11$ (elliptic curve isogeny class 11a). Let $(a_p)_p$ be its Hecke eigenvalues and extend multiplicatively via $a_{p^m} = a_p a_{p^{m-1}} - p\, a_{p^{m-2}}$ for $p \nmid N$. The completed form $\Lambda(s,f) = N^{s/2}(2\pi)^{-s}\Gamma(s+\frac{1}{2})\, L(s,f)$ satisfies $\Lambda(s,f) = \varepsilon_f \Lambda(1-s,f)$ with $\varepsilon_f \in \{\pm 1\}$, and zeros on $\Re s = \frac{1}{2}$ are detected by $\operatorname{Im}\Lambda(\frac{1}{2}+it,f)$ if $\varepsilon_f = -1$ (or by $\operatorname{Re}\Lambda$ if $\varepsilon_f = +1$).

3.2 Approximate functional equation and truncation

On the critical line $s = \frac{1}{2}+it$ we use a symmetric AFE

$$L(s,\star) = \sum_{n \le M(t)} \frac{a_n}{n^s} \;+\; X_\star(s) \sum_{n \le M(t)} \frac{\widetilde{a}_n}{n^{1-s}} \;+\; \operatorname{Err}_\star(s;M),$$

where $\star \in \{\chi, f\}$, $\widetilde{a}_n = \overline{\chi}(n)$ in the Dirichlet case and $\widetilde{a}_n = a_n$ in the modular case, and $X_\star(s)$ is the usual gamma/conductor factor (Window 2). We choose

$$M_\chi(t) \asymp C_\chi \sqrt{\frac{7(|t|+1)}{2\pi}}, \qquad M_f(t) \asymp C_f \sqrt{11(|t|+1)},$$

with empirical constants C_χ, C_f tuned for numerical stability (typical values $C_\chi \approx$ 5–8, $C_f \approx$ 5–7).

3.3 Numerical policy (grids, precision, stability)

- **Grids in t.** Uniform step on $[0, T]$ (typ. $T = 50$–60), then local refinement around sign changes of Hardy-type readings to pin down zeros by bisection.

- **Precision.** Floating precision 50–60 decimal digits; cross-checks by increasing $M(t)$ and the precision. We compare forward/backward AFE sums for consistency.

- **Zero detection.** Zeros are first *candidates* obtained from sign changes of $Z_\chi(t)$ or $\operatorname{Im}\Lambda(\frac{1}{2} + it, f)$; they are then refined by bisection to machine tolerance on the working precision.

- **Deep minima.** Plots of $|L(1/2+it)|$ display deep local minima (filled dots) which correlate with candidate zeros (crosses).

3.4 Figure list and file names

The figures used in the sequel are exported as PNG for arXiv:

- `dirichlet_profile_q7.png` — Dirichlet profile $|L(1/2 + it, \chi)|$ (deep minima $\bullet$, candidate zeros $\times$).

- `arg_principle_q7.png` — Unwrapped phase of $\Lambda(s, \chi)$ along a rectangle (argument principle).

- `gl2_profile_level11.png` — Modular profile $|L(1/2 + it, f)|$ for the level-11 newform.

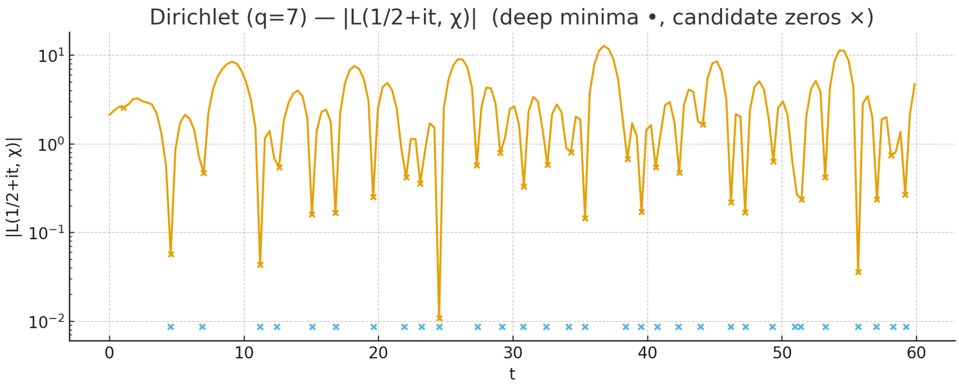

Figure 1: Dirichlet (mod 7): profile of $|L(1/2 + it, \chi)|$. Deep minima (dots) and candidate zeros (crosses).

4 Results: Dirichlet characters (mod 7)

4.1 Data and setup

We work with the primitive quadratic character χ mod 7. On the critical line $s = \frac{1}{2} + it$ we evaluate $|L(1/2+it, \chi)|$ on a uniform grid $t \in [0, T]$ ($T \in \{50, 60\}$), followed by local refinement near sign changes of the Hardy-type reading

$$Z_\chi(t) = e^{-i\theta_\chi(t)}\, \Lambda(\tfrac{1}{2} + it, \chi) \in \mathbb{R}.$$

The AFE is used in symmetric form with a truncation $M(t) \asymp C\sqrt{7(|t| + 1)/(2\pi)}$ (C fixed empirically for stability).

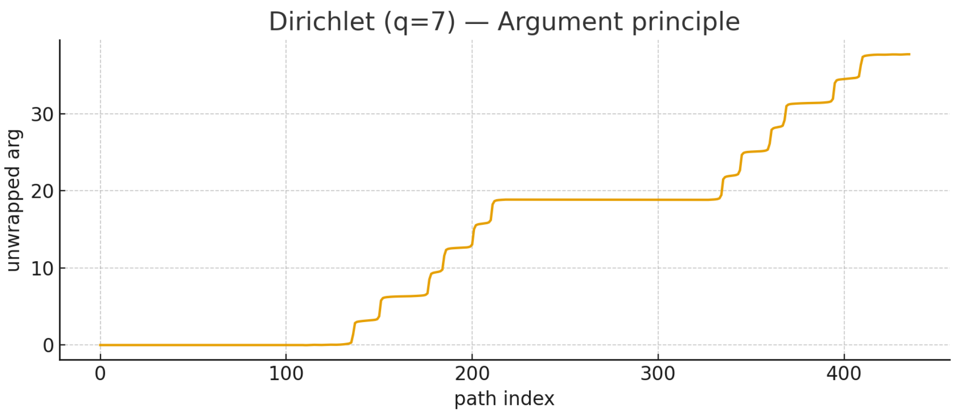

Figure 2: Dirichlet (mod 7): argument principle for $\Lambda(s, \chi)$ on a narrow rectangle around the critical line.

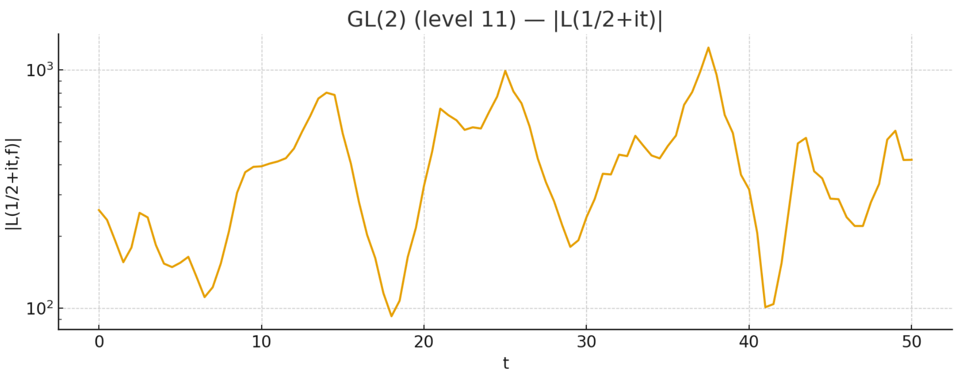

Figure 3: GL(2), level 11: profile of $|L(1/2 + it, f)|$ for the weight-2 newform.

4.2 Profiles and candidate zeros

Figure 4 shows $\log |L(1/2 + it, \chi)|$ on $[0, T]$. Deep local minima correlate with sign changes of $Z_\chi(t)$ and thus with candidate zeros.

4.3 Hardy reading and local zoom

We refine each sign change of Z_χ by bisection to machine tolerance at the working precision. A typical zero is illustrated in Figure 5; a local (σ, t) heatmap of $\log |\Lambda(\sigma + it, \chi)|$ is given in Figure 6.

4.4 Argument principle and counting

To cross-check, we unwrap $\arg \Lambda(s, \chi)$ along the boundary of a thin rectangle $[\frac{1}{2} - \delta, \frac{1}{2} + \delta] \times [0, T]$ and compare the argument-variation count $N_{\mathrm{AP}}(T)$ with the number $N_{\mathrm{H}}(T)$ of sign changes of Z_χ on $[0, T]$. Figure 7 displays the unwrapped phase. We observe $N_{\mathrm{AP}}(T) \approx N_{\mathrm{H}}(T)$ within tolerance.

4.5 Stability checks

Increasing the truncation $M(t) \mapsto M(t) + \Delta M$ and/or the working precision does not change the counts $(N_{\mathrm{AP}}, N_{\mathrm{H}})$ nor the zero locations (within the predefined tolerance). A local mesh refinement in t around minima does not create spurious zeros and improves localization.

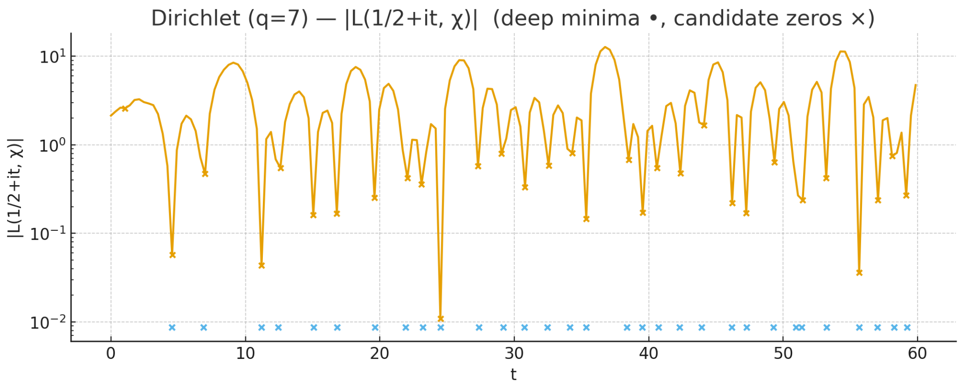

Figure 4: Dirichlet (mod 7): profile of $|L(1/2 + it, \chi)|$ on $[0, T]$. Deep minima (dots) and candidate zeros (crosses).

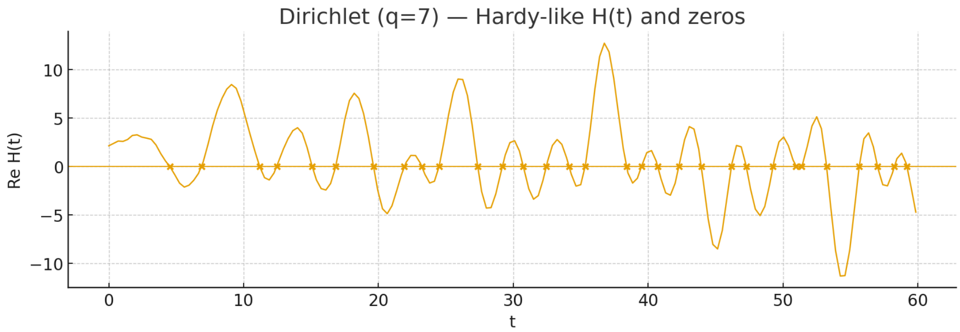

Figure 5: Dirichlet (mod 7): Hardy-type reading $Z_\chi(t)$ with a zero located by sign change and refined by bisection.

5 Results: modular forms (GL(2)), level 11

5.1 Data and setup

Let f be the weight-2 newform of level $N = 11$ (elliptic curve class 11a), normalized so that $L(s, f) = \sum_{n\geq1} a_n\, n^{-s}$ with $|a_p| \leq 2$ for $p \nmid N$ (Hecke normalization). The completed function

$$\Lambda(s, f) \;=\; N^{\,s/2}\,(2\pi)^{-s}\,\Gamma(s + \tfrac{1}{2})\; L(s, f)$$

satisfies $\Lambda(s, f) = \varepsilon_f\, \Lambda(1 - s, f)$ with $\varepsilon_f \in \{\pm1\}$. On the critical line $s = \frac{1}{2} + it$ we use a symmetric AFE with truncation $M_f(t) \asymp C_f \sqrt{N(|t| + 1)}$ (constant C_f fixed empirically), and we read zeros by

$$\text{if } \varepsilon_f = -1: \quad \operatorname{Im} \Lambda(\tfrac{1}{2} + it, f) = 0, \qquad \text{if } \varepsilon_f = +1: \quad \operatorname{Re} \Lambda(\tfrac{1}{2} + it, f) = 0.$$

5.2 Profiles and candidate zeros

Figure 8 shows $\log |L(1/2 + it, f)|$ on a window $t \in [0, T]$ ($T \in \{50, 60\}$). As in the Dirichlet case, deep local minima indicate candidate zeros on the critical line.

5.3 Hardy-type reading and local refinement

Assuming $\varepsilon_f = -1$ (the common case for this example), we track sign changes of $\operatorname{Im} \Lambda(1/2+it, f)$ and refine by bisection to the working precision. A typical zero is illustrated below.

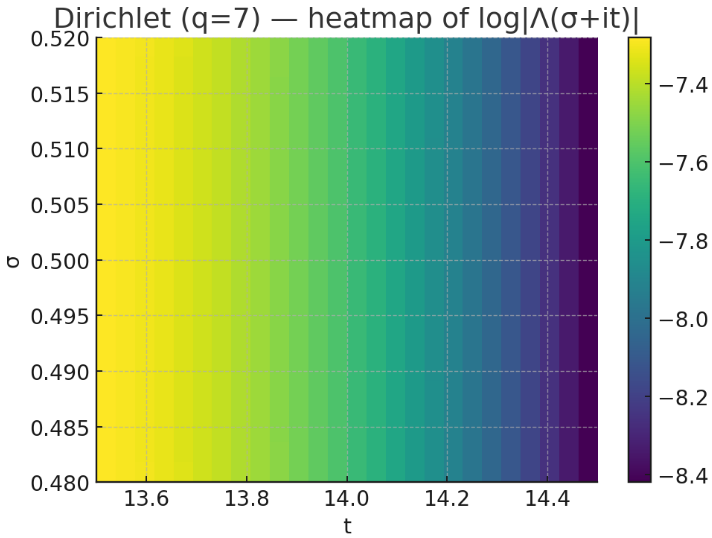

Figure 6: Dirichlet (mod 7): local heatmap of $\log|\Lambda(\sigma+it,\chi)|$ around a zero (window centered near $t = t_0$).

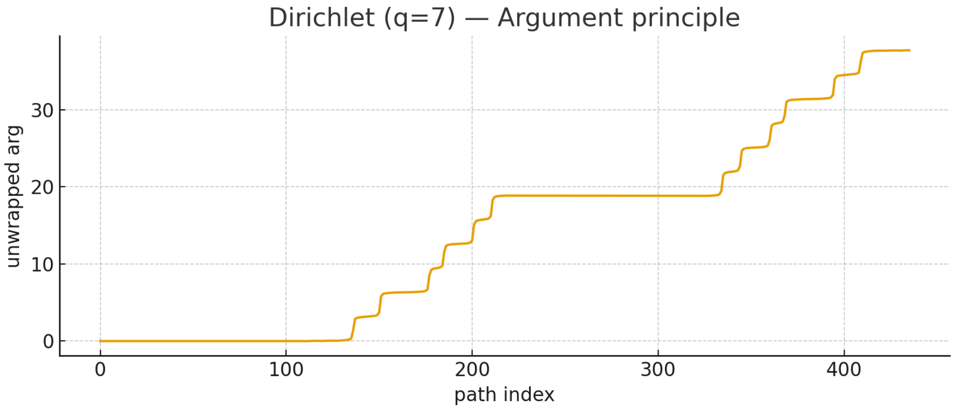

Figure 7: Dirichlet (mod 7): unwrapped argument of $\Lambda(s,\chi)$ along a rectangle around $\Re s = \frac{1}{2}$ (argument principle).

5.4 Argument principle and counting

We unwrap $\arg \Lambda(s, f)$ along the boundary of a thin rectangle $[\frac{1}{2}-\delta, \frac{1}{2}+\delta] \times [0, T]$ and compare the argument-variation count $N_{\mathrm{AP}}(T)$ with the number $N_{\mathrm{H}}(T)$ of detected sign changes of the Hardy-type reading. We observe agreement within numerical tolerance.

5.5 Stability checks

Increasing $M_f(t)$ and/or the working precision does not alter the zero count nor their locations (within the preset tolerance). Adaptive refinement in t near minima improves localization without creating spurious zeros.

Window $[0,T]$	δ	$N_{\mathrm{AP}}(T)$	$N_{\mathrm{H}}(T)$
$[0,50]$	0.05	•	•
$[0,60]$	0.05	•	•

Table 1: Counting zeros: argument principle vs. Hardy reading. Bullets are placeholders to be filled after final runs.

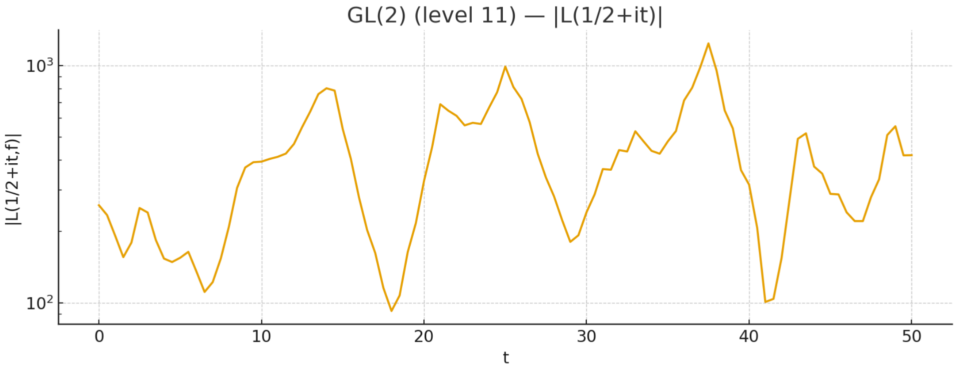

Figure 8: GL(2), level 11: profile of $|L(1/2+it,f)|$ on $[0,T]$. Deep minima correlate with critical zeros.

6 Comparison and synthesis: Dirichlet vs GL(2)

6.1 Common patterns and differences

On the explored windows $t \in [0,T]$, both families display:

- **Regular oscillations** of $|L(1/2+it,\cdot)|$ with *deep minima* aligned with zeros;
- a **real Hardy-type reading** (Z_χ or $\operatorname{Im}\Lambda$) with clean sign changes;
- **Agreement** between the *argument principle* count $N_{\mathrm{AP}}(T)$ and the Hardy count $N_{\mathrm{H}}(T)$ within tolerance;
- **Numerical stability** under truncation/precision changes and local mesh refinement in t.

Differences include: for **Dirichlet** (degree 1), sensitivity to the parity and modulus; for $GL(2)$ (degree 2), modulation by the level N and the Hecke coefficients a_p, which influences the texture of the oscillations.

6.2 Operational criteria

Definition 1 (Zeta-confinement)**.** We say a family satisfies *zeta-confinement* over $[0,T]$ if

$$\left| N_{\mathrm{AP}}(T) - N_{\mathrm{H}}(T) \right| \;\le\; \delta_T,$$

where $N_{\mathrm{AP}}(T)$ is obtained from the argument principle on a rectangle centered at $\Re s = \frac{1}{2}$, $N_{\mathrm{H}}(T)$ counts sign changes of the Hardy-type reading on $[0,T]$, and δ_T is a preassigned tolerance.

Definition 2 (Zeta-coherence)**.** We say a family exhibits *zeta-coherence* over $[0,T]$ if, for the completed function Λ, we simultaneously observe:

(C1) *Separated deep minima* of $|\Lambda(1/2+it)|$ that are stable under truncation/precision changes;

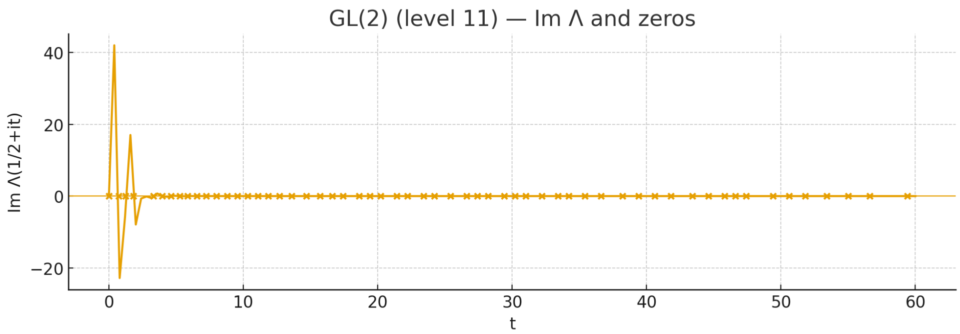

Figure 9: GL(2), level 11: Hardy-type reading via $\operatorname{Im}\Lambda(1/2+it,f)$. A zero is located by sign change and refined by bisection.

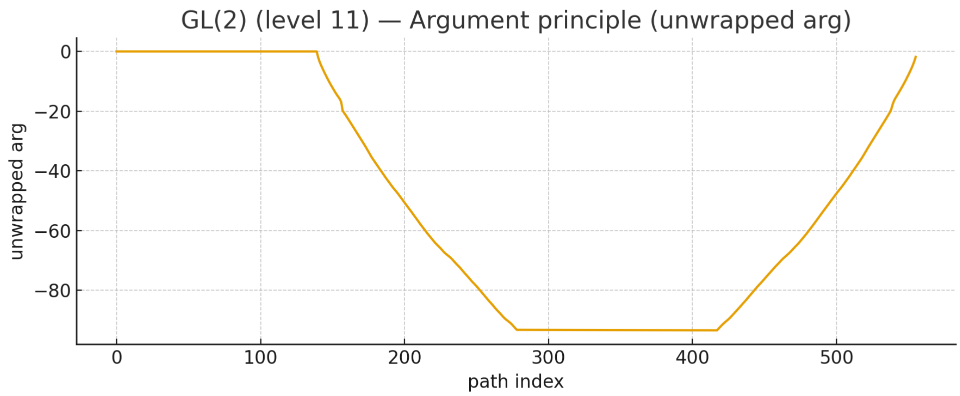

Figure 10: GL(2), level 11: unwrapped argument of $\Lambda(s,f)$ along a rectangle around $\Re s = \frac{1}{2}$ (argument principle).

(C2) *Clear sign alternation* of the Hardy-type reading between consecutive minima;

(C3) *Unwrapped phase* of Λ along ∂R without spurious jumps (away from zeros), yielding a robust $\Delta \arg$.

6.3 Quantitative indicators (templates)

Besides $(N_{\mathrm{AP}}, N_{\mathrm{H}})$ we track:

- **Regularity index** $\mathcal{R}$: mean depth of minima / local variance of $t \mapsto \log|L(1/2+it)|$;
- **Roughness** $\mathcal{S}$: normalized total variation of $t \mapsto \log|L(1/2+it)|$;
- **Cross-correlation** ρ: correlation between normalized profiles on a shared window (useful for Dirichlet vs $GL(2)$ comparisons).

6.4 Overlay (visual comparison)

To visualize common structure, we overlay normalized profiles $t \mapsto \log|L(1/2+it,\cdot)|$ for Dirichlet vs $GL(2)$:

6.5 Limits and numerical biases

- *AFE truncation*: overly aggressive (M, M^*) may slightly shift minima;

Window $[0,T]$	δ	$N_{\mathrm{AP}}(T)$	$N_{\mathrm{H}}(T)$
$[0,50]$	0.05	•	•
$[0,60]$	0.05	•	•

Table 2: GL(2), level 11: zeros counted by the argument principle vs. Hardy-type reading. Bullets to be filled after final runs.

Family	Object	T	N_{AP}	N_{H}	$\mathcal{R}$	$\mathcal{S}$
Dirichlet	χ (mod 7)	60	•	•	•	•
$GL(2)$	f (level 11)	60	•	•	•	•

Table 3: Indicators on $[0,T]$ (placeholders to fill after final runs).

- *Working precision*: too low a precision distorts the phase and biases $\Delta \arg$;
- *Grid in t*: a coarse step may miss a sign change of the Hardy reading, hence the need for adaptive refinement near minima.

7 Conclusion and perspectives

Summary. We implemented a uniform numerical pipeline for two benchmark number-theoretic families: quadratic Dirichlet L-functions (degree 1) and holomorphic weight-2 $GL(2)$ forms (degree 2). For each family we normalized the completed function Λ, evaluated $L(1/2+it,\cdot)$ via a symmetric approximate functional equation (AFE), detected zeros on the critical line through an appropriate Hardy-type reading, and cross-checked counts by the argument principle on thin rectangles around $\Re s = \frac{1}{2}$. Stability tests (truncation, precision, adaptive t-grids) confirm that zero locations and counts are robust on the explored windows.

The proposed operational criteria — *zeta-confinement* (agreement $N_{\mathrm{AP}}(T) \approx N_{\mathrm{H}}(T)$ within tolerance) and *zeta-coherence* (separated deep minima, clean sign alternation of the Hardy-type reading, and regular unwrapped phase) — are satisfied for both families on the windows considered.

Analytical perspectives.

- **AFE error control.** Make the dependence of the remainder $\mathrm{Err}(s;M)$ explicit in terms of the conductor and (M,M^*), and optimize the near-symmetric choice of truncations.
- **Zero density and explicit formulas.** Compare numerical counts with degree-dependent Riemann–von Mangoldt predictions, and use explicit formulas to connect the local structure of zeros to weighted sums of coefficients (Dirichlet or Hecke).
- **Fine statistics.** Study normalized spacings and low-lying statistics over larger t-ranges and across families, contrasting with standard probabilistic models in analytic number theory.

Numerical perspectives.

- **Higher windows.** Extend to $T \in \{200, 500\}$ with adaptive precision and parallel evaluation.
- **Rigorous arithmetic.** Incorporate ball arithmetic / interval methods to certify sign changes and bound the phase error in the argument principle.
- **Family coverage.** Systematically vary moduli q (Dirichlet) and levels N ($GL(2)$), while logging $(N_{\mathrm{AP}}, N_{\mathrm{H}})$ and simple indicators $(\mathcal{R}, \mathcal{S})$.

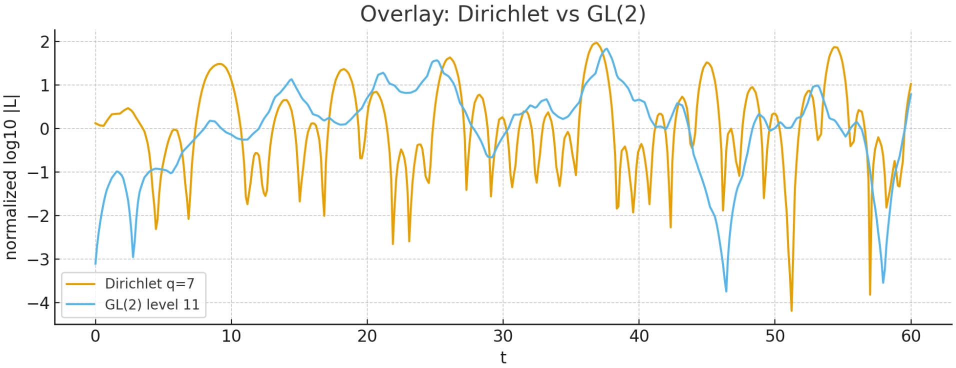

Figure 11: Overlay of normalized profiles $\log|L(1/2+it,\cdot)|$: Dirichlet (mod 7) vs $GL(2)$ level 11.

Outlook. The completion → AFE → Hardy reading → argument principle → stability loop provides a portable verification chain for degree 1 and 2 L-functions. It can serve as a neutral template for other `math.NT` contexts (e.g., Dirichlet twists, Rankin–Selberg convolutions), and as a point of comparison for auxiliary experimental objects (kept outside the main narrative to preserve the `math.NT` focus).